Supplementary Information-I for

Investigation of Nonadiabatic Dynamics in Photolysis of Methyl Nitrate (CH_3ONO_2) by On-the-fly Surface Hopping Simulation

Juanjuan Zhang[†‡], *Jiawei Peng*[†‡], *Deping Hu*[†‡*], *Zhenggang Lan*[†‡*]

[†]SCNU Environmental Research Institute, Guangdong Provincial Key Laboratory of Chemical Pollution and Environmental Safety & MOE Key Laboratory of Environmental Theoretical Chemistry, South China Normal University, Guangzhou 510006, China

[‡]School of Environment, South China Normal University, Guangzhou 510006, China

*E-mail: zhenggang.lan@m.scnu.edu.cn; zhenggang.lan@gmail.com(ZL);
hudp1990@gmail.com(DH)

S1. Electronic-Strucuture Calculations

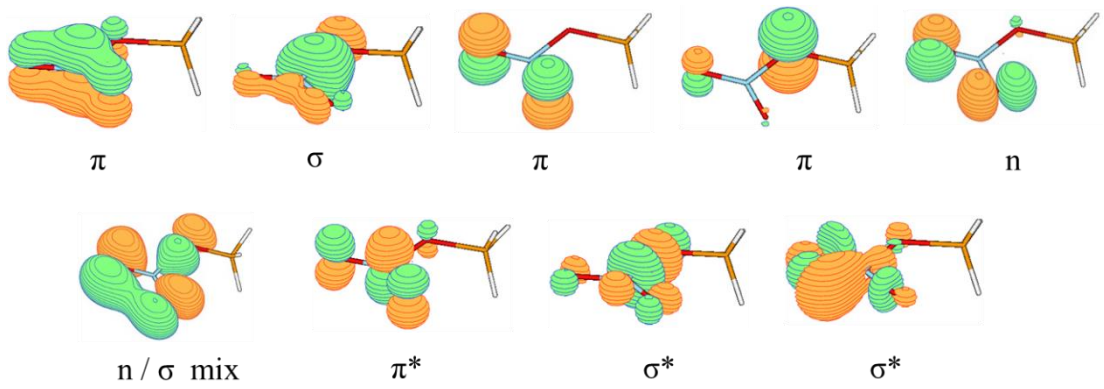

Figure S1: Active space orbitals in the XMS(4)-CASPT2(12,9)/def2-SVPD calculations. The same active space was used in the SA (4)-CASSCF(12,9) calculations.

Table S1. Important geometrical parameters at S_0-min and S_1-min.

	$\mathbf{r_a}$(Å)	$\mathbf{r_b}$(Å)	$\mathbf{r_c}$(Å)	$\mathbf{r_d}$(Å)	$\mathbf{r_e}$(Å)	$\boldsymbol{\theta_a}$(°)	$\boldsymbol{\tau_a}$(°)
S_0-min	1.42	2.25	2.18	1.21	1.20	130.0	0
S_1-min	1.39	2.32	2.23	1.27	1.32	109.0	26.8

Table S2. Relative energies (eV) at the S_0-min, S_1-min, and MECIs.

state	S_0	S_1	S_2	S_3
S_0-min	0	4.84	5.76	6.54
S_1-min	2.06	3.74	5.54	7.27
CI_{10}-I	1.91	1.93	5.94	5.97
CI_{10}-II	3.92	3.93	4.52	4.54
CI_{10}-III	4.45	4.57	5.38	5.48
CI_{21}-I	4.38	4.42	4.61	4.71
CI_{21}-II	5.60	5.61	5.61	5.62
CI_{21}-III	4.21	4.33	4.33	4.45
CI_{21}-IV	4.93	5.01	5.39	5.41
CI_{32}-I	2.31	4.52	5.87	6.01
CI_{32}-II	4.48	4.50	4.69	4.72
CI_{32}-III	3.65	3.67	4.39	4.41
CI32-IV	2.24	2.34	5.35	5.48
CI_{32}-V	3.32	3.44	7.60	7.72

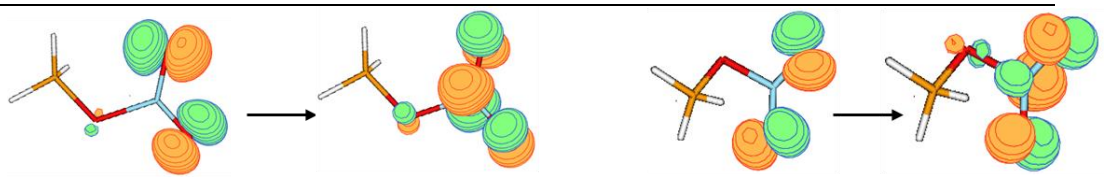

Figure S2: The transition orbitals of the S_1 state of S_0-min (a) and S_1-min (b).

Table S3. Critical geometrical parameters at MECIs.

CIs	r_a(Å)	r_d(Å)	r_e(Å)	θ_a(°)	τ_a(°)
CI_{10}-I	3.11	1.21	1.17	133.5	81.2
CI_{10}-II	3.19	1.16	1.45	110.3	90.4
CI_{10}-III	1.35	1.44	1.30	95.1	34.2
CI_{21}-I	2.84	1.63	1.14	109.6	72.8
CI_{21}-II	1.35	1.19	3.76	79.9	28.3
CI_{21}-III	2.91	1.13	1.83	108.8	72.7
CI_{21}-IV	1.36	1.37	1.37	95.0	40.9
CI_{32}-I	1.32	1.55	1.28	123.4	1.0
CI_{32}-II	3.05	1.13	1.71	109.3	98.1
CI_{32}-III	3.12	1.35	1.22	109.2	106.5
CI_{32}-IV	3.13	1.23	1.23	131.8	103.5
CI_{32}-V	3.09	1.18	1.20	169.2	0.3

S2. CI-Seams

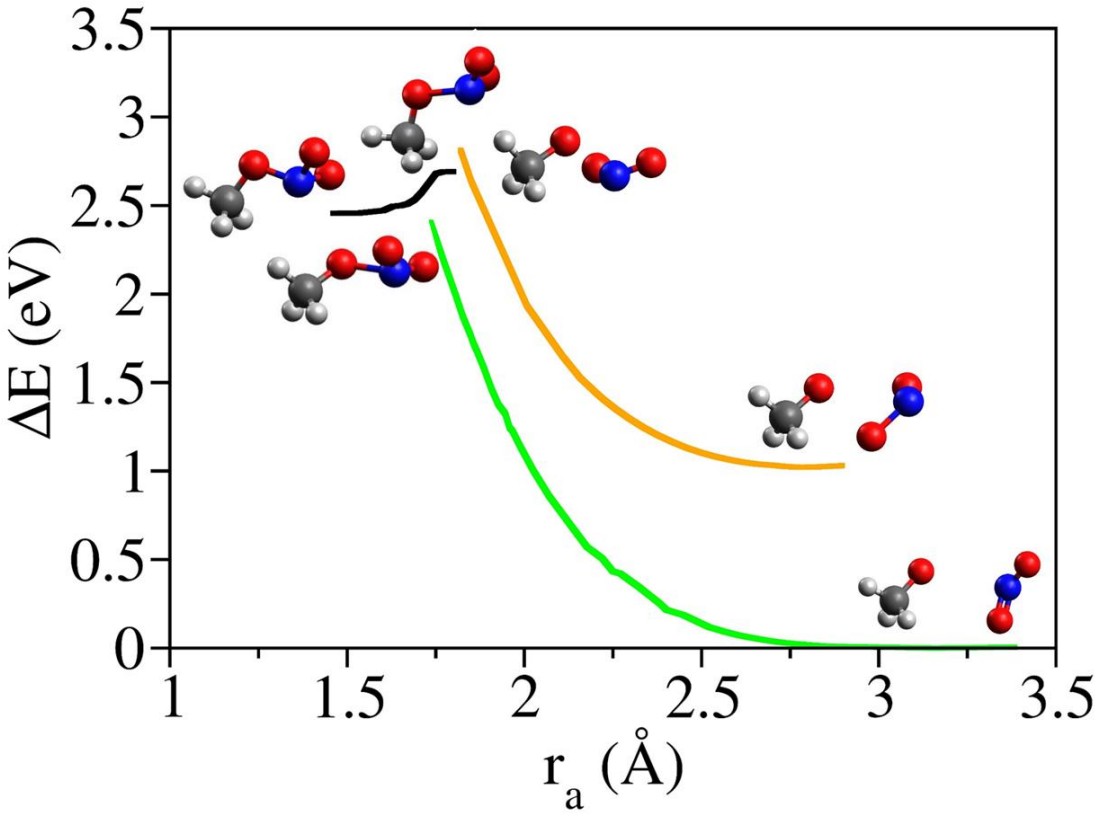

Figure S3: Energies of the S_1-S_0 CI_{10}-seams along with the bond r_a: CI_{10}-seam-I (green line); CI_{10}-seam-II (orange line); CI_{10}-seam-III (black line). The CI_{10}-seams were calculated with the constrained optimization at the SA(2)-CASSCF(12,9)/def2-SVPD level. For comparison, the minimum-energy geometry of CI_{10}-seam-I was set as zero.

S3. Typical Trajectories

Here the representative trajectories towards to different photolysis channels are given in Figure S4-S7. We show the total energy, kinetic energy, and all involved potential energies for the representative trajectories before the S_1-S_0 hops, see Figure S4-S7 (a). This shows that energy conservation is basically acceptable before the nonadiabatic decay to the ground electronic state. After the internal conversion to the ground state, the electronic-structure problems may take place at any time due to the highly-distorted geometries, and energy conservation may not strictly be satisfied. However, the excessive energy anyway pushes the system towards the dissociation limit, where the quasi-degeneracy of low-lying electronic states exists due to symmetry reasons. This can be viewed by the energy difference in the dissociation limit, see Figure S4-S7 (b).

Typical trajectories passing CI_{10}-I, CI_{10}-II, and CI_{10}-III were discussed in Figure S4, S5, and S6, respectively. In all above channels, the photolysis products are only $CH_3O + NO_2$, and two lowest states may become nearly degenerated in the dissociation limit. The $CH_3O + NO + O$ channel does not play an major role in the dynamics starting from S_1, while this channel becomes important when the trajectories are initialized from a higher state. Figure S7 shows a typical trajectory of this channel, which starts from S_3. Note that four lowest electronic states become almost degenerated in the dissociation limit.

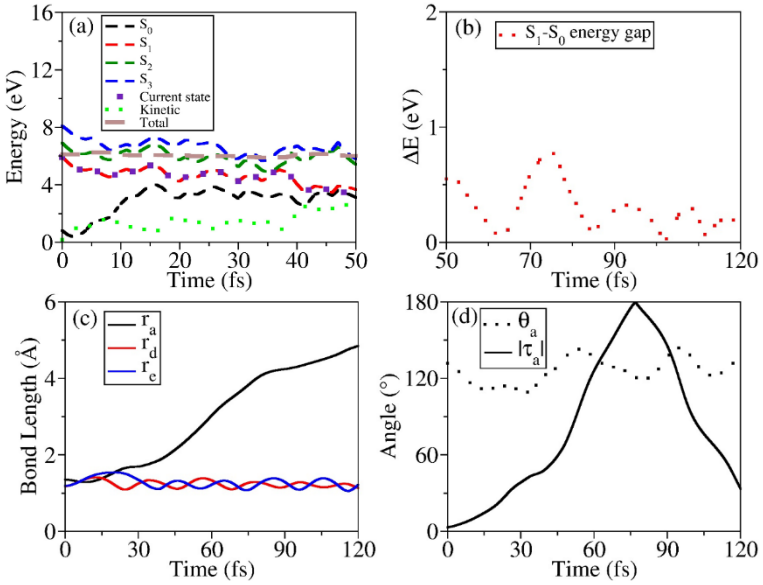

Figure S4: Time-dependent properties of a typical trajectory initialized from S_1 via the CI_{10}-I: (a) potential energies of relevant electronic states, total, and kinetic energies before S_1-S_0 hops; (b) energy gaps between S_1 and S_0 towards the $CH_3O + NO_2$ channel; (c–d) geometric parameters (c): r_a, r_d, and r_e, (c): θ_a and τ_a as functions of simulation time.

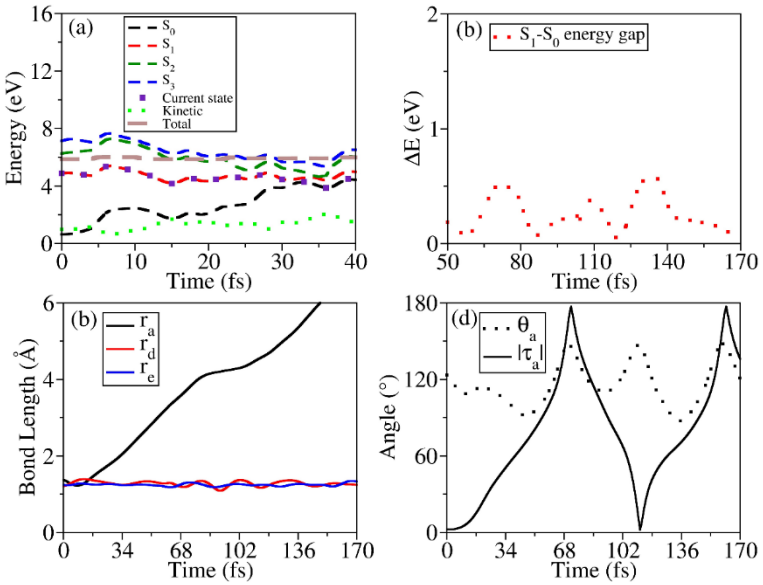

Figure S5: Time-dependent properties of a typical trajectory initialized from S_1 via the CI_{10}-II: (a) potential energies of relevant electronic states, total, and kinetic energies before S_1-S_0 hops; (b) energy gaps between S_1 and S_0 towards the $CH_3O + NO_2$ channel; (c–d) geometric parameters (c): r_a, r_d, and r_e, (d): θ_a and τ_a as functions of simulation time.

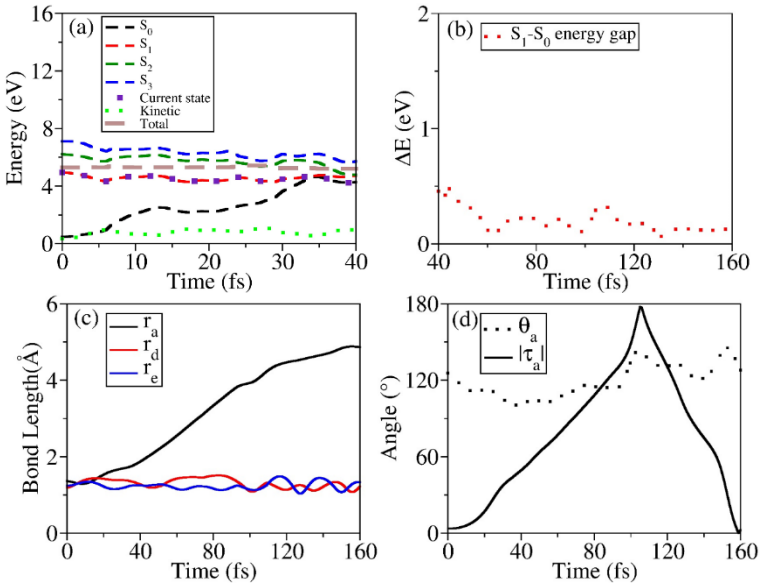

Figure S6: Time-dependent properties of a typical trajectory started from S_1 via CI_{10}-III: (a) potential energies of relevant electronic states, total, and kinetic energies before S_1-S_0 hops; (b) energy gaps between S_1 and S_0 towards the $CH_3O + NO_2$ channel; (c–d) geometric parameters (c): r_a, r_d, and r_e, (d): θ_a and τ_a as functions of simulation time.

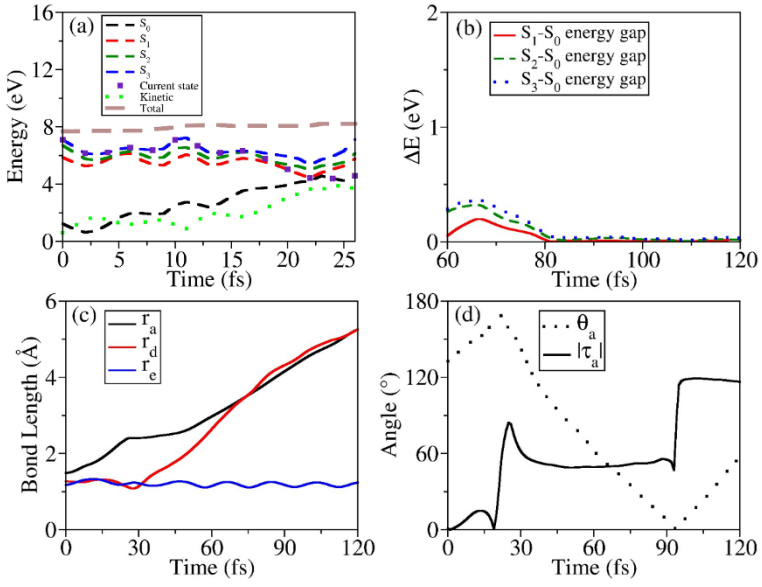

Figure S7: Time-dependent properties of a typical trajectory initialized from S_3 via CI_{10}-III: (a) potential energies of relevant electronic states, total, and kinetic energies before S_1-S_0 hops; (b) energy gaps of S_1 and S_0, S_2 and S_0, and S_3 and S_0, respectively towards the $CH_3O + NO + O$ channel; (c–d) geometric parameters (c): r_a, r_d, and r_e, (d): θ_a and τ_a as functions of simulation time

S4. Additional Results of the TSH Dynamics from S_2 and S_3

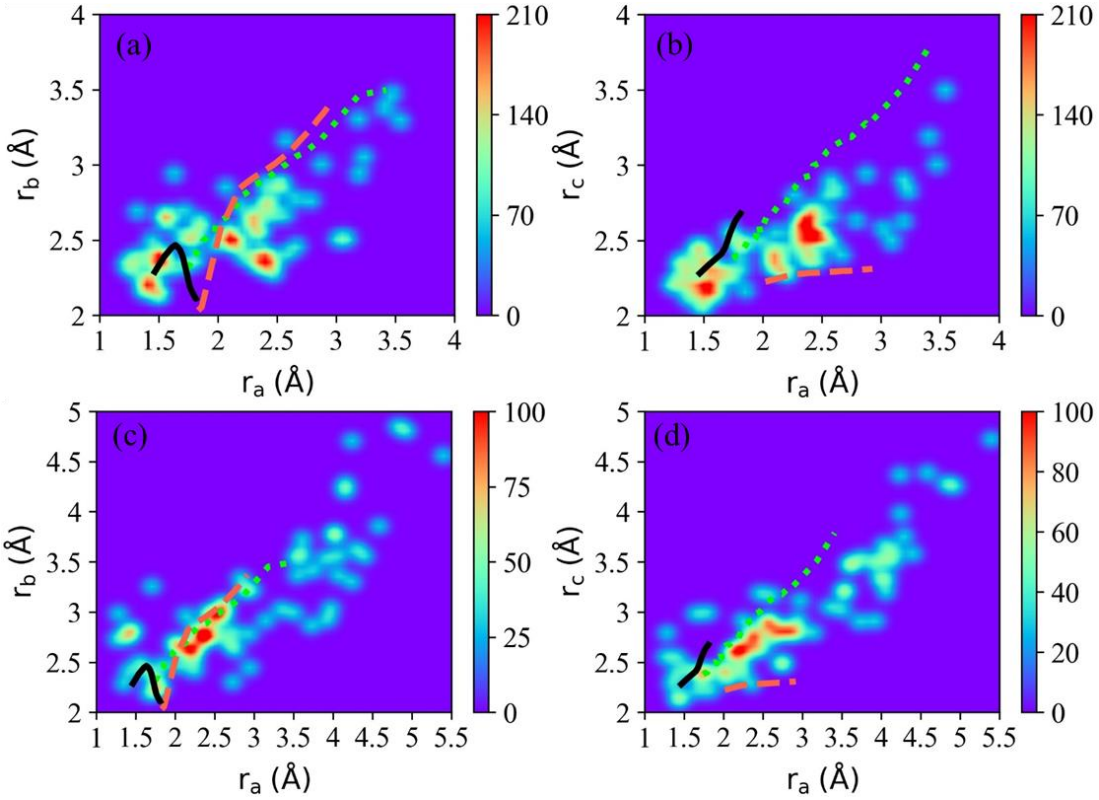

Figure S8: Distribution of the important geometric parameters at the first S_1 to S_0 hops within 80 fs: (a) and (b): initiated from S_2 state; (c) and (d): initiated from S_3 state. In all panels, the green dotted line, orange dashed line, and black solid line marks the CI_{10}-seamI, CI_{10}-seamII, and CI_{10}-seamIII, respectively.

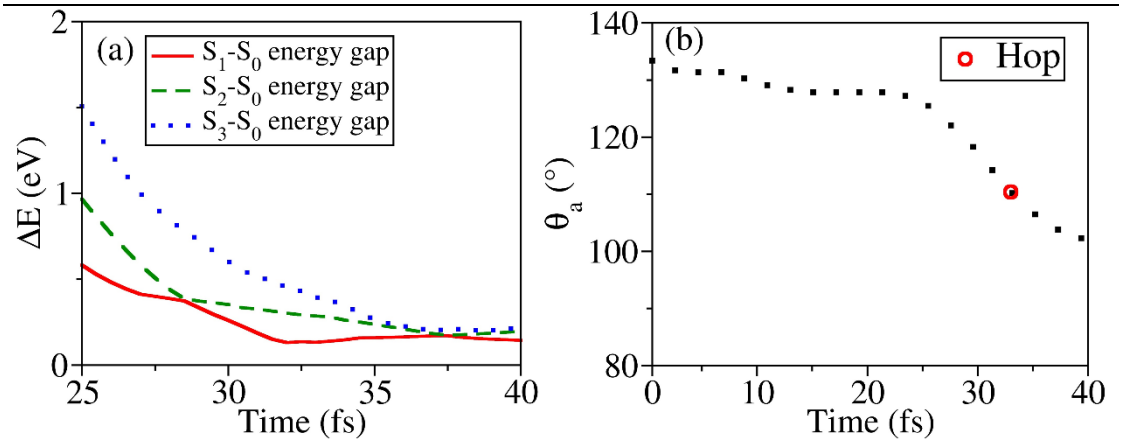

Figure S9: Time-dependent properties of a typical trajectory initialized from S_3 state displays degeneracy at hops: (a) energy gaps of S_1 and S_0, S_2 and S_0, and S_3 and S_0, respectively towards the $CH_3O + NO_2$ channel; (b) geometric parameters θ_a as functions of simulation time.